JCSE The Journal of Corrosion Science and Engineering

ISSN 1466-8858

Volume 7 Paper 3

# Cu-Ni-Zn-Mn Alloys for Sulphide Polluted Seawater Applications

A.P.Patil* and Dr. R.H. Tupkary

Department of Metallurgical and Materials Engineering, Visvesvaraya National Institute of Technology, Nagpur – 440 011 (India), Email: appatil14@yahoo.co.uk

## Abstract

Cu-10Ni alloy suffer from accelerated corrosion in sulphide polluted seawater. New copper base alloy containing 10% Ni, 29% Zn and, 3% and 5% Mn have been developed and tested vis-a vis Cu-10Ni alloy in synthetic seawater both clean and polluted with sulphide ions. It is found that Cu-10Ni-29Zn-5Mn and Cu-10Ni-29Zn-3Mn alloys have better corrosion resistance in both the test solutions. Observed behaviour in synthetic seawater is attributed to modification of defective structure of $Cu_2O$ by trivalent cations of Mn. Observed behaviour in sulphide polluted synthetic seawater is attributed to formation of ZnS containing multi-phased film and incorporation of $Mn^{3+}$ in $Cu_2S$ lattice

**Key words**: Copper alloys, Corrosion, Seawater, Sulphide and Film

## Introduction

As a result of excellent corrosion resistance in seawater, 90-10 Cu-Ni has become standard condenser / heat exchanger tube material for seawater applications. However, this alloy suffers from accelerated corrosion in seawater polluted with sulphide. Its poor corrosion resistance in sulphide

polluted seawater is a cause of concern. Like other copper alloys the 90-10 Cu-Ni develops a film of $Cu_2O$, which accords the alloy excellent corrosion resistance in seawater [1]. If seawater is polluted with sulphide, $Cu_2S$ forms in the film [2]. Like the $Cu_2O$ the $Cu_2S$ is a p-type semiconductor but possesses more defective structure than the $Cu_2O$ and thereby causes accelerated corrosion. The accelerated corrosion in sulphide polluted seawater can be mitigated in two ways viz. (i) by modifying defective structure of the $Cu_2S$ and the $Cu_2O$ and (ii) by modifying composition of the film altogether. The defective structure of the $Cu_2O$ is modified when multi-valent cations originating from the alloy get incorporated in its lattice [3]. This improves ionic and electronic resistance of the film and consequently improves corrosion resistance of the alloy. This is achieved by alloying Cu-Ni alloys with Fe, Mn, Al and Cr. These alloying additions produce bi-valent or tri-valent cations like $Ni^{2+}$, $Fe^{2+}$, $Fe^{3+}$, $Mn^{2+}$, $Mn^{3+}$, $Al^{3+}$ and $Cr^{3+}$. Examples of these are, (i) additions of 1-1.8% Fe and 0.5-1% Mn in alloy C70600, (ii) additions of 2% each of Fe and Mn in alloy C71640, (iii) additions of 0.5% Fe, 0.2-1% Mn and 2-3% Cr in alloy C71900, (iv) additions of 0.7-1.2% Fe, 3.5-5.5% Mn, 1-2% Al and 0.5% Cr in alloy C72420 and, (v) additions of 1-2% Fe, 4.5% Mn, 0.5% Cr and 1.9% Al in MARINEL. However structure of $Cu_2S$ seems to be too defective to be modified effectively with these alloying additions.

Certain alloying additions modify the composition of the film and instead of a single-phased film of $Cu_2O$, either a multi-phased film or a single-phased film of some other compound is formed. Examples of such additions are (i) Al addition which produces a film of $Al_2O_3$ (as in Aluminium brass-C86700 and Aluminium bronze-C95800) and (ii) Sn addition which produces a film of SnO2 (as in AP bronze). Films of $Al_2O_3$ and $SnO_2$ accord better corrosion resistance than film of $Cu_2O$ and thereby improve corrosion resistance of the alloys. It is known that addition of Zn improves resistance to sulphide attack as in case of single-phase Cu-Zn alloy but data is scanty. The formation of ZnS, which is a bad conductor, probably accords better resistance to sulphide attack. However, role of Zn addition to Cu-Ni alloy remains to be investigated. Role of Mn in Cu-Ni system is found to be secondary to that of Fe [4] but its role in Cu-Ni-Zn system remains to be investigated. The present work is an attempt in that direction. Accordingly, it is aimed at developing a

series of single-phased Cu-Ni-Zn-Mn alloys by modifying 90-10 Cu-10Ni with additions of 29% zinc and, 3% and 5% manganese and, testing these alloys vis-à-vis Cu-10Ni alloys for corrosion resistance in synthetic seawater, both clean and polluted with sulphide ions.

## Experimental

The test alloys were prepared in the laboratory. These were melted in graphite crucible, then cast in steel mould (10 x 20 x 300 mm), then annealed (for solutionising) at 900°C for three hours, then cold rolled from 10 mm to 1.2 mm thickness, then annealed at 800°C for 2 hours and finally quenched in water. Actual chemical composition of the test alloys and other relevant information are presented in Table 1.

**Table 1: Actual chemical composition of the test alloys**

| Alloy Designation | Cu | Ni | Zn | Mn | Fe | Theoretical density g/cc | Equivalent weight |
|---|---|---|---|---|---|---|---|
| Cu-10Ni | 89.1 | 9.9 | - | - | 0.95 | 8.916960 | 31.4725 |
| Cu-10Ni-29Zn | 58.5 | 11.5 | 29.0 | - | 0.97 | 8.394599 | 31.68541 |
| Cu-10Ni-29Zn - 3Mn | 55.1 | 11.5 | 29.2 | 3.0 | 1.18 | 8.343905 | 31.55677 |
| Cu-10Ni-29Zn - 5Mn | 54.0 | 11.0 | 29.2 | 4.8 | 0.95 | 8.319759 | 31.46466 |

The alloys possess single-phase microstructure as presented in Fig. 1. Testing for corrosion involved weight loss, cathodic and anodic polarisation methods. Test solutions used in these studies were clean synthetic seawater (SSW) and sulphide polluted SSW. Nominal composition of clean SSW used in this investigation is as per ASTM standard D114-75 (reproved 1980) for synthetic seawater but without heavy metal ions. For preparing sulphide-polluted seawater LR grade $Na_2S$ was added to SSW. In general 0.1 g $Na_2S$ was added to 1 litre SSW. The nominal pH of SSW was 8.2, but changed to 9.2 on addition of $Na_2S$. The pH was then adjusted to 8.2 by addition of 0.05N $H_2SO_4$. It was

found, that almost whole of sulphide ions were oxidised to sulphate in one day. This required the test solution to be replenished daily with sulphide ions. Hence, a fresh solution of $Na_2S$ in SSW was added to the test solution daily and resultant rise in pH was neutralised by addition of 0.05N $H_2SO_4$.

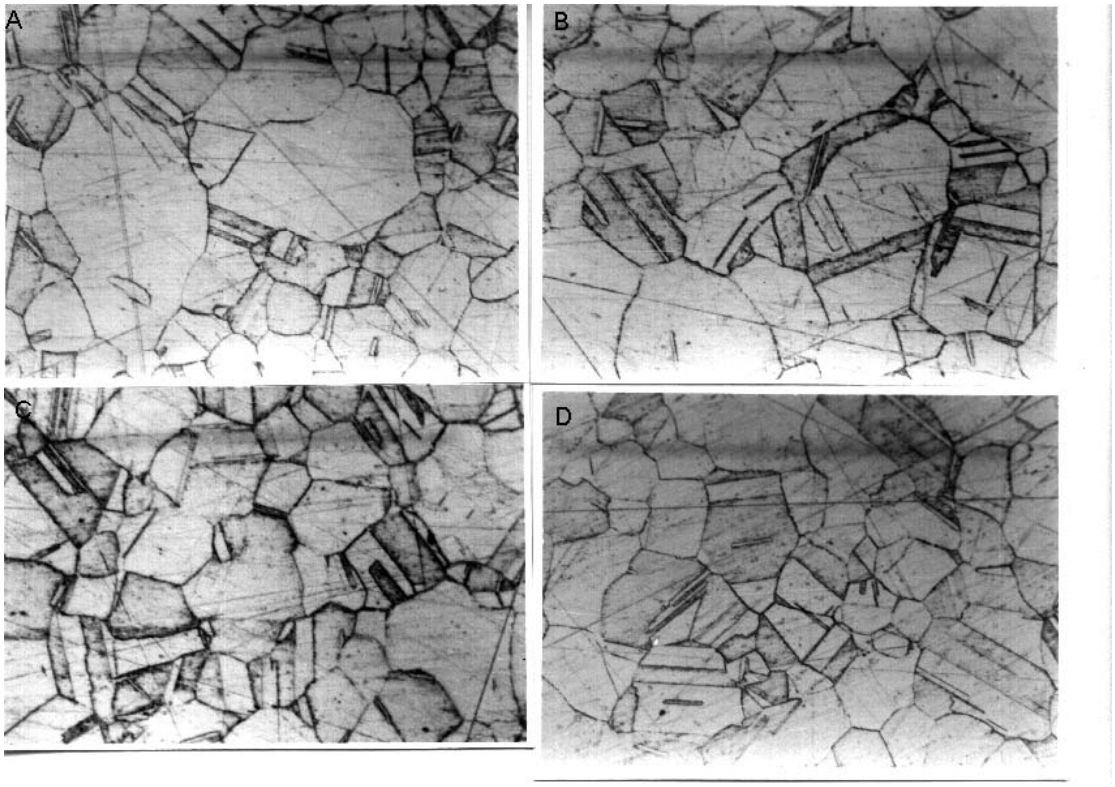


Fig.1: Microstructure of test alloys; showing well developed single-phased grains (A: Cu-10Ni, B: Cu-10Ni-29Zn, C: Cu-10Ni-29Zn-3Mn and D: Cu-10Ni-29Zn-5Mn).

## Weight Loss

Specimens (10 x 25 x 1.2 mm) were cut and prepared by abrading on a series of emery paper (1/0, 2/0, 3/0 and 4/0) for the weight loss tests. Specimens were degreased in 5% NaOH solution and then washed with water just before testing. The pH of SSW was 8.2 and temperature was 27°C. Test duration was 15 days, but to study effect of exposure duration the specimens were taken out at planned intervals of 0-3, 0-6, 0-9, 0-12 and 0-15 days. The corroded specimens were then subjected to cleaning by scrubbing with bristle brush using scourer powder and distilled water. The samples were then washed in distilled water, then rinsed in methanol

and then air dried before weighing for weight loss. One set of Cu-10Ni-29Zn-5Mn specimens was prepared in the same way, then exposed to respective test solutions for 15 days and then subjected to scanning electron microscopy. The films were analysed using EDX attached to SEM (JEOL 840A) and also by XRD (Philips PW1017 based).

### Polarisation

The specimens for polarisation studies were prepared by soldering a piece of insulated copper wire at one flat surface of specimen (10 x10 x1.8 mm). These were then mounted in cold setting resin in such a way that the soldered joint was completely embedded and the other flat surface was open. The open surface was prepared by abrading on series of emery papers (1/0, 2/0, 3/0, 4/0 and 5/0). Polished specimens were then washed with soap and distilled water just before setting up cell. These specimens were allowed to reach a stable open circuit potential (OCP) for almost 30-35 minutes, before carrying out the polarisation test. The OCP of the test alloys was found to be in the range of -50 mV (SHE) to +30 mV (SHE) except that of Cu-10Ni in sulphide polluted SSW being -600 mV (SHE).

Anodic and cathodic polarisation studies were carried out with a three-electrode system using a computer-controlled potentiostat (Sycopel AUTOSTAT 253). Platinum electrode (cylindrical mesh) was used as counter electrode and saturated calomel electrode was used as reference electrode however, all potentials are referenced to Saturated Hydrogen Electrode (SHE). The cathodic polarisation was started from -560 mV (SHE), increased towards OCP and stopped when current became positive. The solution was stirred with a magnetic stirrer to minimise effects of concentration polarisation. The anodic polarisation was started at -60 mV (SHE) and stopped after +500 mV (SHE). The solution was stagnant in anodic polarisation studies. The scan rate in cathodic polarisation was 0.166 mV/s and that in anodic polarisation was 0.08 mV/s.

## Results and Analysis

Figures 2 and 3 present results of weight loss studies in clean and sulphide polluted SSW, respectively and shows the effect of exposure

duration on weight loss and corrosion rate of the test alloys. It is evident that manganese-containing alloys have better corrosion resistance than other two alloys. It is evident that rate of corrosion is high initially and then decreases with increasing exposure duration. It is also evident that rate of change of weight loss is high initially and then tapers down. However, the plots have not reached to a plateau, it means that the rate of corrosion will fall further if the exposure duration is extended beyond 15 days.

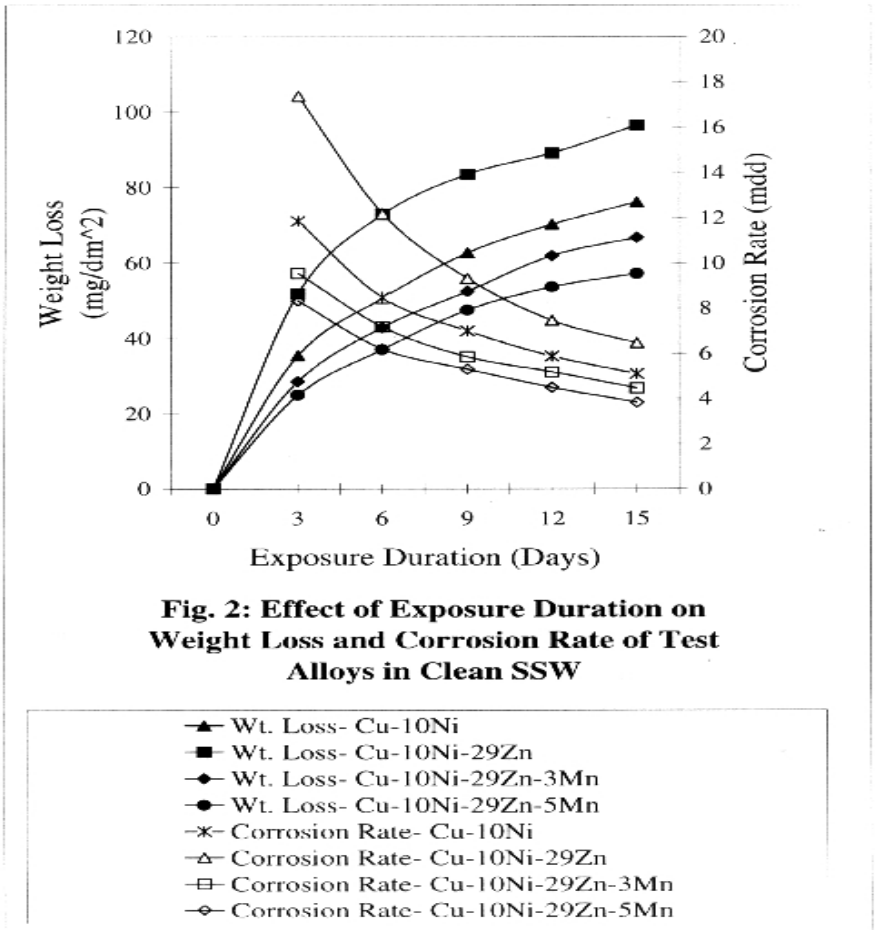


**Fig. 2: Effect of Exposure Duration on Weight Loss and Corrosion Rate of Test Alloys in Clean SSW**

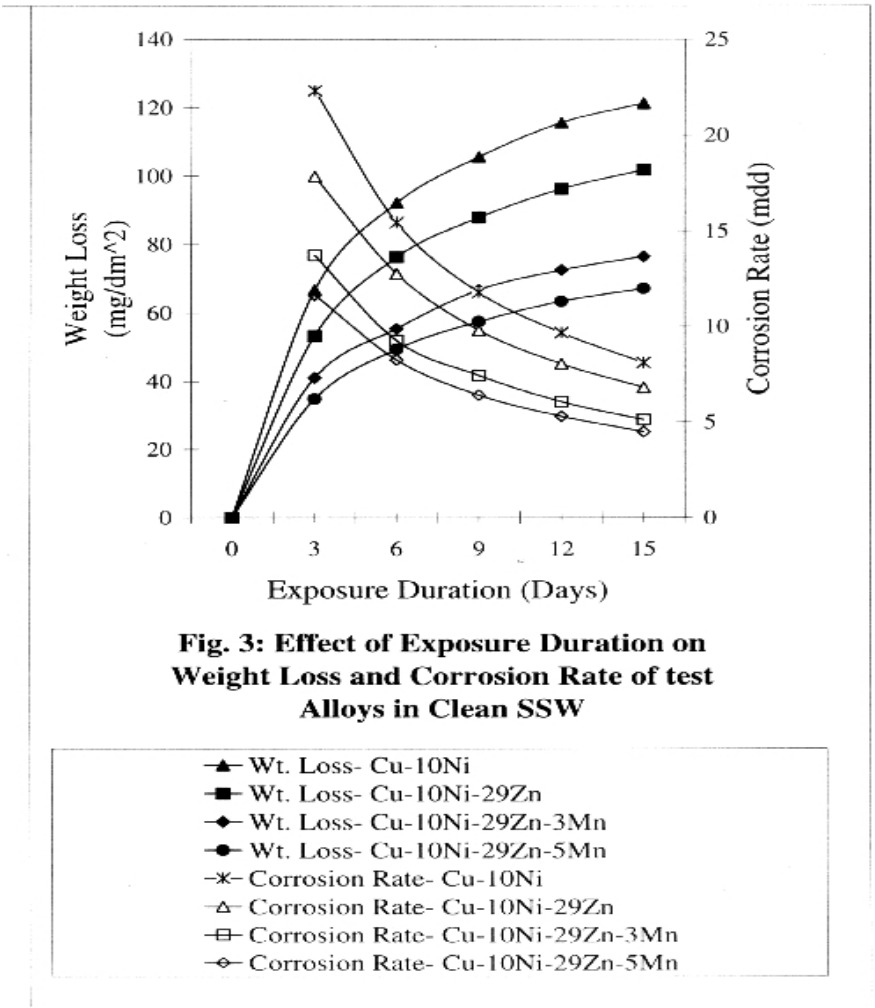


**Fig. 3: Effect of Exposure Duration on Weight Loss and Corrosion Rate of test Alloys in Clean SSW**

Figure 4 presents SEM photomicrographs of the film formed on Cu-10Ni-29Zn-5Mn exposed to clean SSW. It shows that the film covers entire surface and is compact. It also shows that the film is made up of two layers. The inner layer is crystalline and forms the bulk of the film and, the outer layer is powdery. Figure 5 presents SEM photomicrographs of the film formed on Cu-10Ni-29Zn-5Mn in sulphide polluted SSW. It shows that the film covers entire surface but is defective and has many clusters of globular substance.

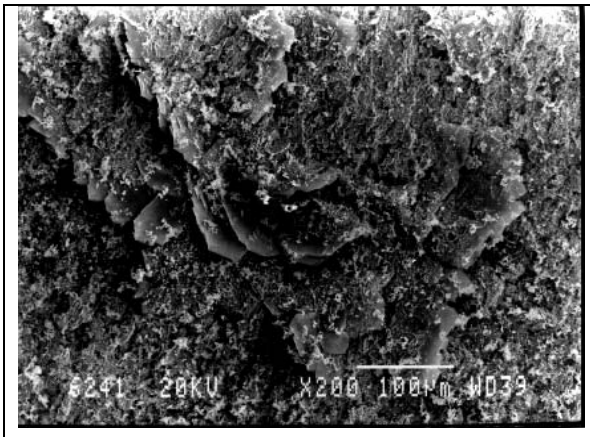


Fig. 4: SEM photomicrograph of the film formed on Cu-10Ni-29Zn-5Mn alloy in clean synthetic seawater.

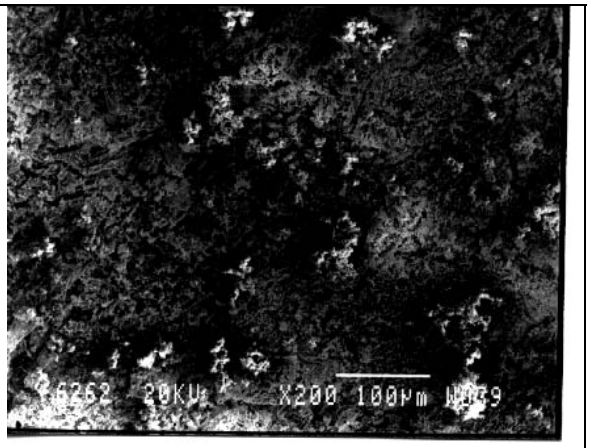


Fig. 5: SEM photomicrograph of the film formed on Cu-10Ni-29Zn-5Mn alloy in sulphide polluted synthetic seawater.

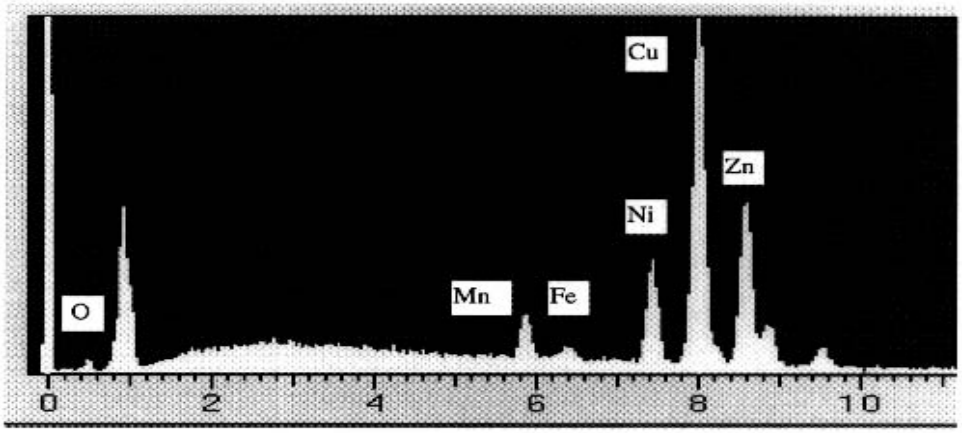


Fig. 6: EDX spectrum of polished surface of Cu-10Ni-29Zn-5Mn alloy

Figure 6 presents EDX spectrums of polished Cu-10Ni-29Zn-5Mn alloy. Various peaks in this figure in general represent composition of the Cu-10Ni-29Zn-5Mn alloy. Whereas, Fig. 7 presents EDX spectrums of the film formed on Cu-10Ni-29Zn-5Mn in clean SSW and Fig. 8 shows EDX spectrums of the base film formed on Cu-10Ni-29Zn-5Mn in sulphide polluted SSW. Comparison of Figs. 6 and 7 indicates that the film formed in clean SSW has alloying elements almost in the same ratio as that in substrate and, has substantial oxygen, sulphur and chlorine. Comparison of Figs. 7 and 8 indicates that the film has large quantity of Zn and small quantities of Cu and Ni and, large quantity of O, S and Cl.

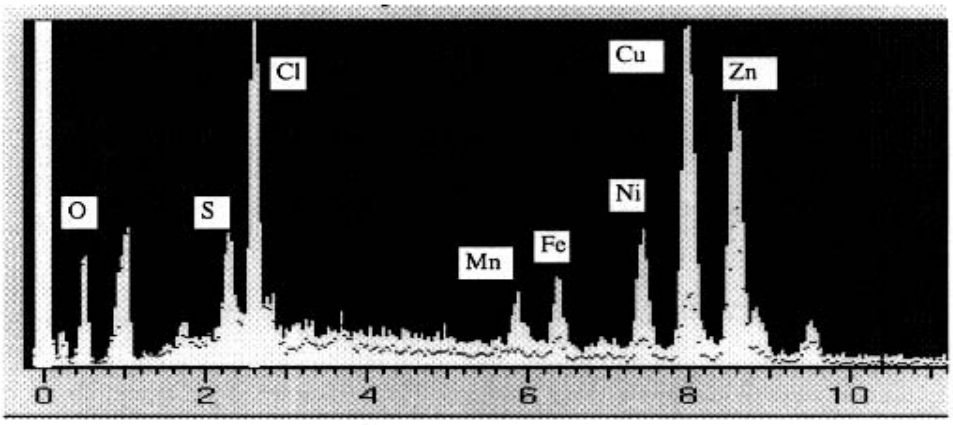


Fig. 7: EDX spectrum of film formed on Cu-10Ni-29Zn -5Mn after 15-days exposure to SSW

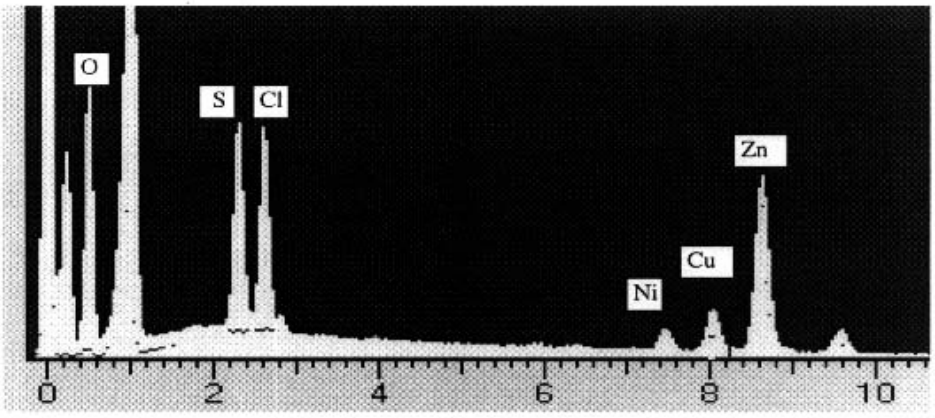


Fig. 8: EDX spectrum of base film seen in film (Fig. 5.233) formed on Cu-10Ni-29Zn -5Mn exposed to SSW+$Na_2S$ for 15 days.

Figure 9 presents XRD spectrum of the polished Cu-10Ni-29Zn-5Mn alloy. The positions of all the peaks match with those of copper, indicating thereby that the alloy is single-phased. These peaks are slightly shifted to left of copper positions, suggesting thereby some strain in the lattice. This lattice strain is attributed to formation of solid solution of alloying elements in the copper. Figure 10 shows XRD spectrum of the alloy corroded in SSW for 15 days. Like Fig. 9, in this figure also the positions of all the peaks match with the copper position. This indicates that the film is coherent with the substrate matrix and is single-phased. The $Cu_2O$ is formed epitaxially and is coherent with the substrate matrix [3]. It therefore suggests that the film formed on Cu-10Ni-29Zn-5Mn in SSW is made of $Cu_2O$. Figure 11 presents XRD spectrum of the film formed on Cu-10Ni-29Zn-5Mn alloy in sulphide polluted SSW. There are many peaks in this figure and therefore it indicates that the film is multi-phased. Out of these peaks, four peaks match with the copper positions

and indicate presence of $Cu_2O$. The remaining peaks indicate presence of oxides and sulphides, although exact identification is not possible owing to non-stoichiometric composition of these oxides and sulfides [5]. It is likely that oxides like $Cu_2O$, CuO, ZnO, NiO and, sulfides like $Cu_2S$, CuS, ZnS and NiS are formed in this film

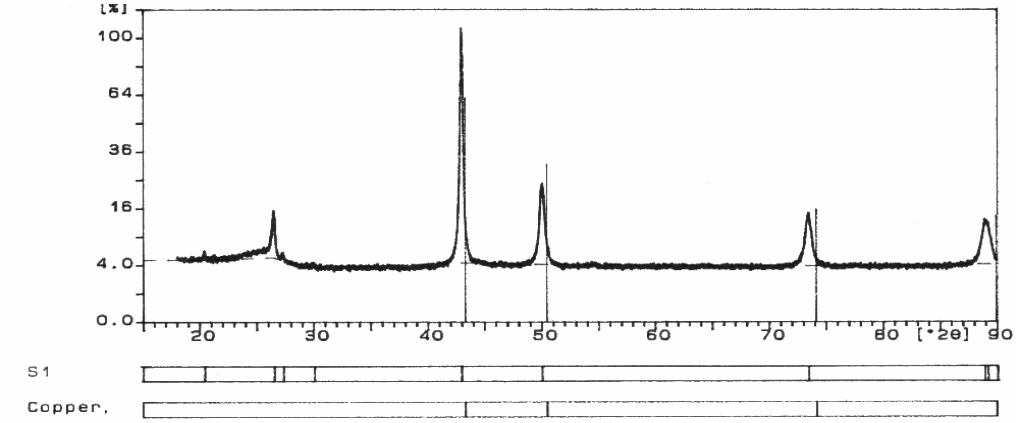


Fig. 9: XRD spectrum of polished specimen of Cu-10Ni-29Zn-5Mn alloy

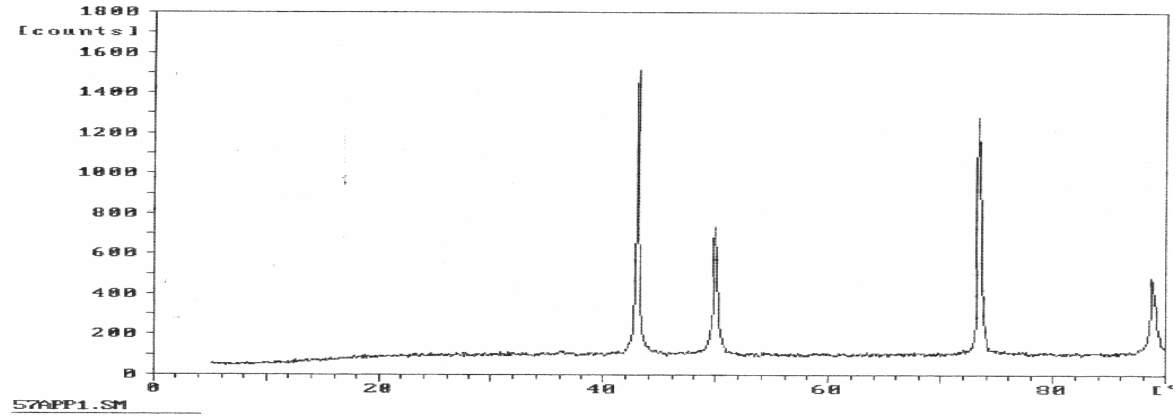


Fig. 10: XRD analysis of film developed on Cu-10Ni-29Zn -5Mn alloy exposed to SSW for 15 days

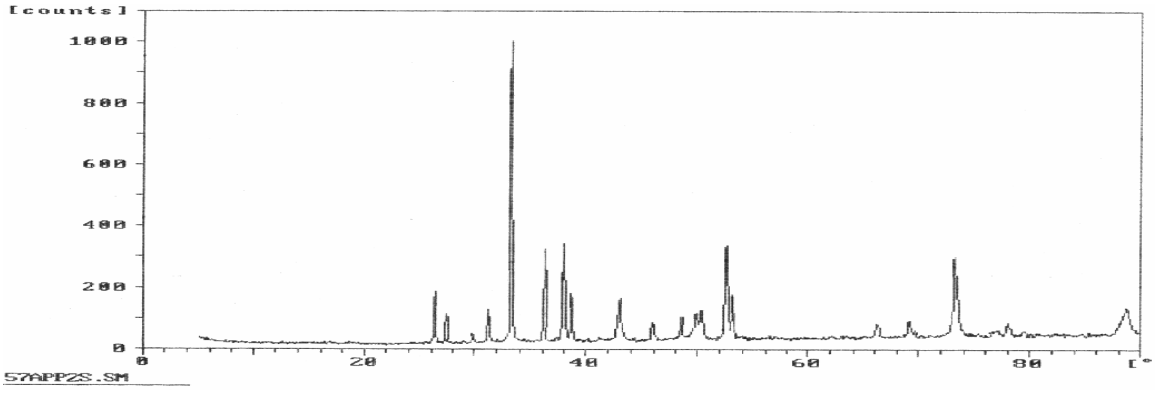

Fig. 11: XRD spectrum of film developed on Cu-10Ni-29Zn -5Mn alloy exposed to sulfide polluted SSW for 15 days

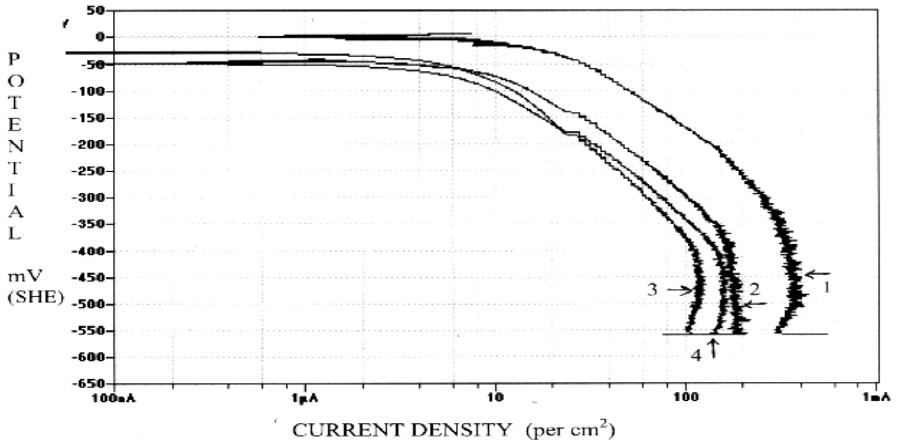


Fig. 12: Cathodic Polarisation Plots of Test Alloys in Clean SSW
1- Cu-10Ni, 2- Cu-10Ni-29Zn, 3- Cu-10Ni-29Zn-3Mn and 4- Cu-10Ni-29Zn-5Mn

Figure 12 presents cathodic polarisation plots of the test alloys in clean SSW. It is seen that Ecorr of all the test alloys is almost in the range of 0 to 50 mV (SHE) although Ecorr of Cu-10Ni alloy is relatively nobler. It is evident that at potential lower than -400 mV (SHE) the cathodic c.d. reaches a limiting value. This indicates that the cathodic reaction is under diffusion control. At potentials higher than -400 mV (SHE) the cathodic plot is near linear. This indicates that the cathodic reaction in this potential range is under activation control. This linear region is extrapolated to obtain icorr. The icorr of Cu-10Ni alloy is higher than other test alloys. The data obtained from these plots is presented in Table 2.

**Table 2: Data obtained from cathodic polarisation vis-à-vis immersion test**

| Alloy | SSW | | | | SSW+Na2S | | | |
|---|---|---|---|---|---|---|---|---|
| | $i_{corr}$ μA/ $cm^2$ | $CR_T$ mdd | Tafel slope βc mV | $CR_W$ mdd | $i_{corr}$ μA/ $cm^2$ | $CR_T$ mdd | Tafel slope βc mV | $CR_W$ mdd |
| Cu-10Ni | 19 | 5.35 | 230 | 5.09 | 50 | 14 | 375 | 8.94 |
| Cu-10Ni-29ZN | 12 | 3.37 | 275 | 6.46 | 40 | 11.2 | 650 | 8.11 |

| | | | | | | | | |
|---|---|---|---|---|---|---|---|---|
| Cu-10Ni-29Zn-3Mn | 10 | 2.8 | 350 | 4.46 | 18 | 5.05 | 400 | 5.12 |
| Cu-10Ni-29Zn-5Mn | 9 | 2.53 | 280 | 3.83 | 15 | 4.2 | 375 | 4.49 |

Where, $CR_T$ = Corrosion rate from Tafel extrapolation and,

$CR_W$ = Corrosion rate from weight loss in immersion test.

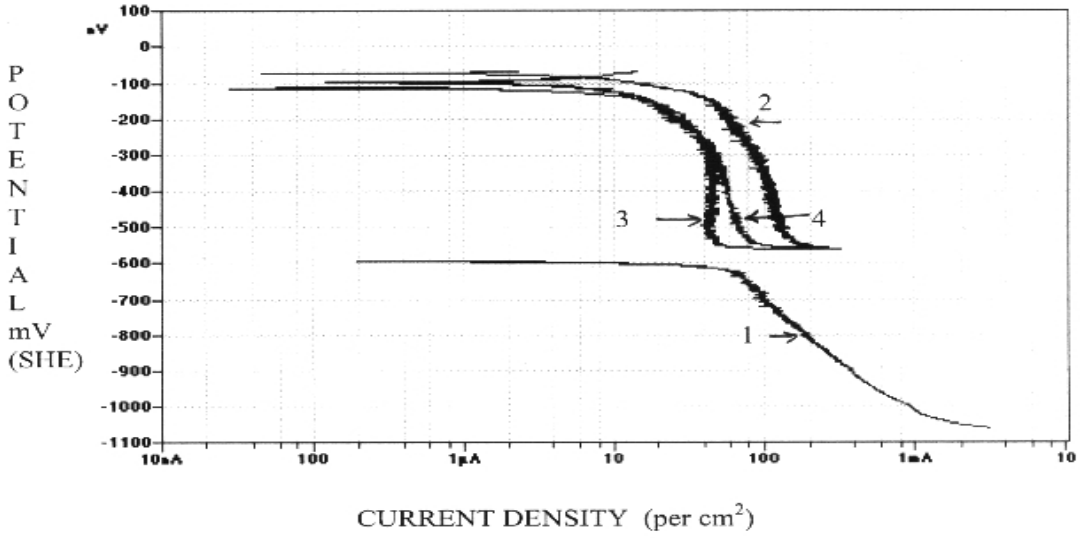


Fig. 13: Cathodic Polarisation Plots of Test Alloys in Sulphide Polluted SSW
1- Cu-10Ni, 2- Cu-10Ni-29Zn, 3- Cu-10Ni-29Zn-3Mn and 4- Cu-10Ni-29Zn-5Mn

Figure 13 presents cathodic polarisation plots of the test alloys in sulphide polluted SSW. From this figure it is evident that the $E_{corr}$ of Cu-10Ni is -600 mV (SHE) and those of other alloys are in the range of -80 to -120 mV (SHE). It is evident that the Cu-Ni-Zn-Mn alloys have relatively much nobler $E_{corr}$ than Cu-10Ni in sulphide polluted SSW. It was noticed that specimens of Cu-10Ni had developed a violet tinge in 30 minutes exposure before the cathodic polarisation test and that the specimen had lost the tinge completely at the end of cathodic polarisation tests. It means that the film that was developed in the initial exposure was reduced in cathodic polarisation. Whereas, the specimens of Cu-Ni-Zn-Mn alloys developed a light golden tinge during initial exposure of 30 minutes and that the specimens retained the tinge even after cathodic polarisation tests. It means that the components of the film were stable in the range of potential in which the polarisation test was conducted. This suggests that the film formed on Cu-10Ni in sulphide polluted SSW was different from that formed on Cu-10Ni-29Zn-5Mn alloy. The data obtained from these plots is also presented in Table 2. In general there

seems to be reasonably good agreement between corrosion rate obtained in weight loss and that from cathodic polarisation.

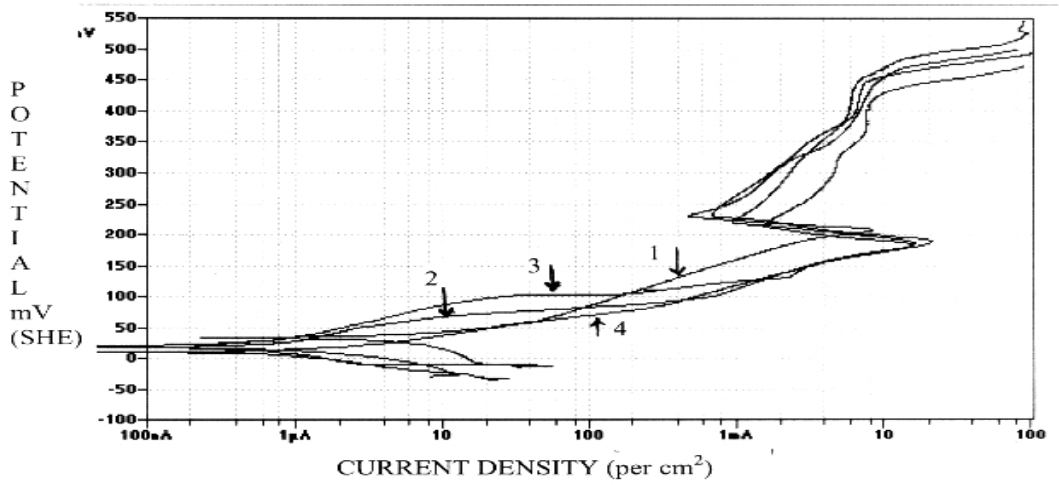


Fig. 14: Anodic Polarisation Plots of \test Alloys in Clean SSW
1- Cu-10Ni, 2- Cu-10Ni-29Zn, 3- Cu-10Ni-29Zn-3Mn and 4- Cu-10Ni-29Zn-5Mn

Figure 14 presents anodic polarisation plots of the test alloys in clean SSW. It is evident that the test alloys undergo rapid active dissolution up to 180-200 mV (SHE) and give a peak c.d. of 10-20 mA/cm$^2$ at this potential. The active dissolution region does not show a well- defined Tafel region and consists of two or more linear regions with different slopes. Milosev and Metikos-Hukovic [6] obtained almost similar active dissolution region in anodic polarisation plots of 90-10 Cu-Ni in borate buffer containing different NaCl concentrations and termed it as 'the apparent Tafel region'. On increasing the potential further the anodic c.d. decreases to approximately 1 mA/cm2. In this region the c.d. is rather limited and increases slowly with increasing potential up to 450 mV (SHE), after which film breaks down. Anodic polarisation plots of commercial Cu-9.4Ni-1.7Fe alloy in air-saturated 3.4 wt% NaCl solution obtained by Kato and coworkers [7] had similar features. Their plots had limiting current region with c.d. of 1-2 mA/cm$^2$ following a peak c.d. of 2 mA/cm$^2$. They termed the observed limiting current region as 'brightening region'. In view of relatively higher c.d. of 1-2 mA/cm$^2$ and almost equal peak c.d. (2 mA/cm$^2$) it was appropriate for them to mention this region as 'brightening region'. But in present study, the c.d. drops noticeably from a peak value of 10-20 mA/cm$^2$ to 0.8-1 mA/cm$^2$ for Cu-10Ni-29Zn-5Mn in SSW. The drop in c.d. is too substantial to be

termed as ‘brightening’ region. Secondly metal is supposed to exhibit passivity when passivation c.d. (ip) is lower than corrosion c.d. (icorr) obtained from cathodic polarisation (Tafel extrapolation). The icorr for Cu-10Ni-29Zn-5Mn in SSW is 9 μA/cm$^2$. Considering this icorr value, c.d. of 1 mA/cm2 is too high for this region to be termed as passive region. In a way this situation lies in between ‘passivity’ and ‘brightening’. Therefore, this passivity is termed as ‘pseudo-passivity’.

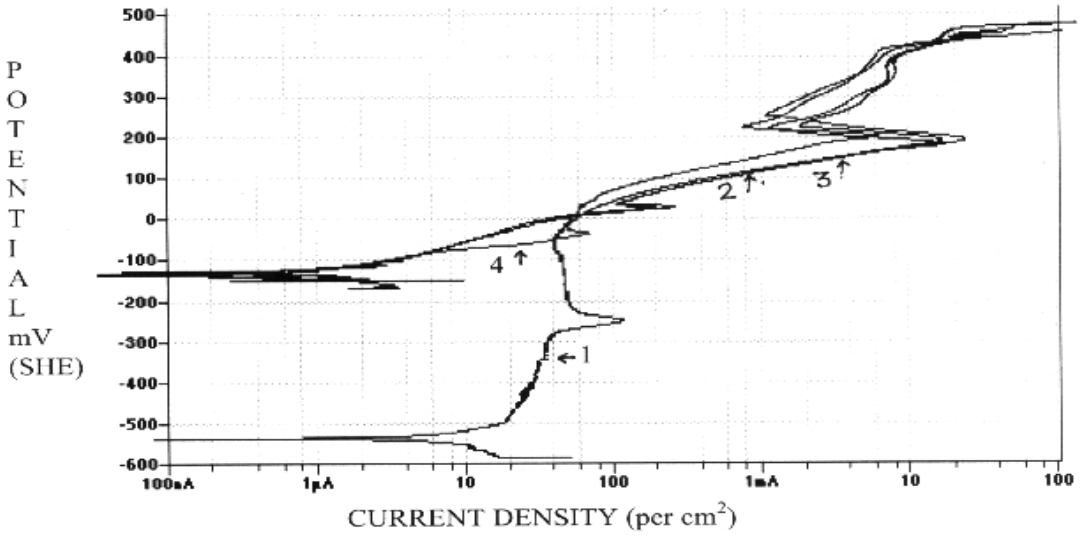


Fig. 15: Anodic Polarisation Plots of Test Alloys in Sulphide Polluted SSW
1- Cu-10Ni, 2- Cu-10Ni-29Zn, 3- Cu-10Ni-29Zn-3Mn and 4- Cu-10Ni-29Zn-5Mn

Figure 15 presents anodic polarisation plots of the test alloys in sulphide polluted SSW. Anodic polarisation plots of test alloys in SSW+$Na_2S$ exhibit two pseudo-passive regions. For example in plot of Cu-10Ni-29-5Mn first region starts at -37 mV (SHE) and second region starts at 181 mV (SHE). The c.d. in first region is 70 μA/cm$^2$ and that in second region is 16 mA/cm$^2$ whereas, $i_{corr}$ is 15 μA/cm$^2$. Considering the $i_{corr}$ of 15 μA/cm$^2$, the c.d. in first region is too high for this feature to be termed as passivity. Therefore, this feature is termed as primary pseudo-passivity. Accordingly, these anodic polarisation plots can be divided in three main regions: (i) the apparent Tafel region or free corrosion region, (ii) the primary pseudo-passive region and (iii) the pseudo-passive region. The slope of apparent Tafel region is denoted by dE/dlog(i). Anodic polarisation plots obtained in present investigation for Cu-10Ni is similar

to the plots obtained by Alhaji and Reda [8] for 90-10 Cu-Ni alloy in natural seawater.

Table 3: Data obtained from anodic polarisation plots

| Alloy and solution | $E_{corr}$ mV (SHE) | AnodicTafel Slope $\beta a$ (mV) |
|---|---|---|
| Cu-10Ni in clean SSW | 33 | 75 |
| Cu-10Ni-29Zn in clean SSW | 10 | 50 |
| Cu-10Ni-29Zn-3Mn in clean SSW | 10 | 30 |
| CU-10Ni-29Zn-5Mn in clean SSW | 9 | 18 |
| Cu-10Ni in sulphide polluted SSW | -534 | 700 |
| Cu-10Ni-29Zn in sulphide polluted SSW | -130 | 100 |
| Cu-10Ni-29Zn-3Mn in sulphide polluted SSW | -128 | 100 |
| Cu-10Ni-29Zn-5Mn in sulphide polluted SSW | -134 | 40 |

The data ($E_{corr}$ and Tafel slope) obtained from anodic polarisation plots is presented in Table 3. Comparison of cathodic and anodic Tafel slopes indicate that corrosion of the test alloys in clean SSW is under cathodic control. It also indicates that corrosion of zinc containing alloys in sulphide polluted seawater is also under cathodic control but that of Cu-10Ni alloy in sulphide polluted seawater is under anodic control.

## Discussions

The pH of the test solutions was 8.2 therefore hydrogen reduction reaction would require operating potential lower than -484 mV (SHE).

While, oxygen reduction reaction would require operating potential lower than +0.743 mV (SHE). The open circuit potentials (OCP) of the test alloys were in the range of -50 to +32 mV (SHE). Therefore oxygen reduction reaction will certainly occur, but hydrogen reduction reaction will not occur during free corrosion of these alloys. In SSW+Na2S solution, OCP of Cu-10Ni was -500 mV (SHE), i.e. lower than -484 mV (SHE). But even in this case hydrogen reduction should not occur at OCP because of lack of overvoltage required for this reaction to occur. Hence, in general oxygen reduction reaction was the only possible cathodic reaction in the system under study.

Formation of $Cu_2O$ by direct anodic reaction and cations by oxidation reactions is possible

$$2Cu + 2OH^- \rightarrow Cu_2O + H_2O + 2e \quad (1)$$

$$Cu \rightarrow Cu^+ + e \quad (2)$$

Out of the alloying elements added to the test alloys, Ni and Zn produce bivalent cations and, Fe and Mn produce bivalent and trivalent cations. Table 4 shows the redox potentials for the formation of various cations and the ionisation potentials of these cations.

Table 4: Redox potentials and ionisation potentials of ions of alloying elements

| Cation | Ionisation reaction | Redox potential V (SHE)# | Ionisation potential eV |
|---|---|---|---|
| $Ni^{2+}$ | $Ni^{2+} + 2e^- \rightarrow Ni$ | -0.423 | 35.19 |
| $Zn^{2+}$ | $Zn^{2+} + 2e^- \rightarrow Zn$ | -0.9397 | 39.72 |
| $Mn^{2+}$ | $Mn^{2+} + 2e^- \rightarrow Mn$ | -1.356 | 33.66 |
| $Mn^{3+}$ | $Mn^{3+} + 2e^- \rightarrow Mn$ | -0.401 | 51.2 |
| $Fe^{2+}$ | $Fe^{2+} + 2e^- \rightarrow Fe$ | -0.617 | 30.65 |
| $Fe^{3+}$ | $Fe^{3+} + 2e^- \rightarrow Fe$ | -0.1545 | 54.8 |

# Estimated value assuming cation concentration to be $10^{-6}$ g-ion/litre.

Open circuit potentials of the test alloys were found to be ranging from -50 to 32 mV (SHE) in SSW. Therefore, $Mn^{3+}$, $Fe^{3+}$, $Ni^{2+}$, $Zn^{2+}$, $Fe^{2+}$ and $Mn^{2+}$ cations are stable species. It is reported that Ni is present as $Ni^{2+}$ and Fe is present as $Fe^{3+}$ ion in the film of $Cu_2O$ formed on 90-10 Cu-Ni alloy [3]. The stability of $Mn^{3+}$ ion is more than that of $Fe^{3+}$ ion, owing to ionisation potential (51.2eV) and redox potential (-0.401 V (SHE)) of $Mn^{3+}$ being lower than those of $Fe^{3+}$ (54.8eV and -0.1545 V (SHE), respectively). Therefore $Mn^{3+}$ will certainly form.

North and Pryor [3] found the $Cu_2O$ and $Cu_2(OH)_3Cl$ to be forming on Cu, Cu-10Ni-1Fe-0.5Mn and Cu-30Ni-0.4Fe in boiling NaCl solution. Kato and coworkers [7] studied the mechanism of corrosion of Cu-9.4Ni-1.7Fe alloy in air saturated NaCl solution. They found by XRD analysis that the corrosion product developed on the surface of Cu-Ni alloy had $Cu_2O$ and $Cu_2(OH)_3Cl$. In both the cases the inner layer formed by direct anodic reaction and outer layer by precipitation. The inner layer was $Cu_2O$ and outer layer was $Cu_2(OH)_3Cl$. The film formed on Cu-10Ni-29Zn-5Mn shown in Fig. 4 too has two layers, crystalline inner layer and powdery outer layer. XRD analysis has indicated that this film is made of single-phased $Cu_2O$. The ionic and electronic resistivities of such a composite film would depend upon resistivities of these individual layers. The $Cu_2O$ is a metal-deficient p-type semiconductor [3]. Various anions and cations entering the film affect ionic and electronic resistivities of $Cu_2O$. Incorporation of cations having valency more than one increases ionic and electronic resistivities of $Cu_2O$. Whereas, incorporation of anions like $Cl^-$ and $OH^-$ decreases the ionic and electronic resistivities of $Cu_2O$. The cations enlisted in Table 4 originating from substrate can modify the defect structure and therefore improve corrosion resistance accorded by the $Cu_2O$ film.

The incorporation of $Ni^{2+}$ ions in the $Cu_2O$ film has been reported to increase ionic and electronic resistivities of the $Cu_2O$ film forming on 90-10 and 70-30 Cu-Ni alloys [3]. In the similar manner incorporation of $Ni^{2+}$ ions in the $Cu_2O$ film forming on test alloys should improve ionic and electronic resistivities of the film. Since, nickel is added to all the test

alloys in equal quantities hence, no specific relative effect of nickel can be highlighted for these alloys. But, it is natural that nickel would contribute to ionic and the electronic resistance of the film. Trivalent cations of Fe are going to be more effective than bivalent ions in increasing ionic and electronic resistivities. This is so because, when one $Fe^{3+}$ ion replaces $Cu^{+}$ ion in the $Cu_2O$ lattice, it increases two positive charges. This rise in positive charges requires incorporation of two electrons to maintain charge neutrality. Incorporation of two electrons in the $Cu_2O$ lattice annihilates two positive holes and consequently shall increase electronic resistivities. If trivalent cation of Fe occupies a vacant position in the lattice then it would be even more effective. This is as per findings of North and Pryor [3] that the rise in the electronic resistivity for $Ni^{2+}$ ions entering the $Cu^{+}$ vacancy is $2.2x10^{8}$ ohm.cm and that for $Ni^{2+}$ ions replacing $Cu^{+}$ is $1.1x10^{8}$. Considering the fact that diffusion of $Cu^{+}$ ions in the $Cu_2O$ lattice takes place via vacancy-assisted mechanism, in which vacancies move inward and $Cu^{+}$ ions move outward. Drop in number of vacant sites due to placement of $Fe^{3+}$ ion in place of $Cu^{+}$ ion in the lattice makes cationic movement that more difficult and consequently increases ionic resistivity.

The test alloys have varying quantity of Mn therefore it is expected that proportional quantity of $Mn^{3+}$ be incorporated in the film. It is expected that incorporation of $Mn^{3+}$ in $Cu_2O$ lattice is as effective as the incorporation of $Fe^{3+}$ is. In that event it should increase ionic and the electronic resistance of the film with increasing manganese content and this effect should manifest itself in polarisation plots. It has been found to be so in cathodic and anodic polarisation studies of test alloys. Cathodic polarisation plots of the filmed specimens have been found to shift to lower current density with increasing manganese content. Similarly, $i_{crit}$ have been found to decrease with increasing manganese content in anodic polarisation plots of polished specimens. The effect of manganese is more pronounced in cathodic polarisation than in anodic polarisation. This is consistent with the findings of North and Pryor [3], who found the ionic resistivity of the $Cu_2O$ film to increase by 4.5 times and the electronic resistivity by 6.5 times on three fold increase in nickel content of Cu-Ni alloys (from 10wt% to 30wt%). Therefore, corrosion resistance of Cu-10Ni-29Zn-3Mn and Cu-10Ni-29Zn-5Mn alloys being

better than Cu-10Ni is attributed to single-phased $Cu_2O$ film and incorporation of bi-valent and trivalent ions of Mn.

Traverso et al.[9] found MxSy type sulfide of alloying elements when Cu-30Ni-2Fe-2Mn allot was exposed to natural seawater containing 8 ppm sulphide. In the similar way the film formed in SSW+$Na_2S$ solution is likely to contain sulphides of alloying elements. The estimated redox potential for the formation of $Cu_2S$, ZnS and MnS are -0.88 V, -1.46 V and -1.52 V, respectively (considering 1 $gl^{-}$ $Na_2S$ = 41 ppm $S^{2-}$). The OCP of zinc containing alloys was -50 mV (SHE) or higher thus, it is natural that these sulphides would form. Secondly solubility product of $Cu_2S$ ($1.9x10^{-48}$) is relatively lower than those of ZnS ($3.2x10^{-25}$) and MnS ($5x10^{-14}$). Therefore, $Cu_2S$ should always be the first compound to form. However, considering the fact that Zn is surface-active element and that ZnS has more negative redox potential (-1.46 V) than $Cu_2S$ (-0.88 V), simultaneous formation of ZnS and $Cu_2S$ is possible. The ionic and electronic resistivities of the overall film depend upon its structure and phases. The ZnS is a bad conductor and when it forms as a separate phase in any part of film, it will not allow electronic and ionic conduction. If few grains of ZnS are formed then it will reduce the area of the film through which ionic and cationic conduction can take place. In that event the corrosion rate of the test alloys should be lower. This is what has been found out in the present studies in case of zinc-containing alloys. Besides, incorporation of various ions in the lattices of different phases may also affect resistivity of the film. The $Cu_2S$ is p-type semiconductor and its lattice is more metal-deficient than that of $Cu_2O$ [8]. Therefore, the resistivity of the $Cu_2S$ shall always be less than that of $Cu_2O$ if similar cations are incorporated in similar quantities. In this way the corrosion resistance of Cu-10Ni alloy should be relatively lower in sulphide polluted SSW than other alloys. This has been found in the present investigation. However, incorporation of $Mn^{3+}$ ions in the $Cu_2S$ lattice would improve its ionic and electronic resistance. Therefore, Mn containing alloys should show better corrosion resistance than Cu-10Ni. This has been found to be so in the present investigation.

## Conclusions

The Cu-10Ni-29Zn-5Mn and Cu-10Ni-29Zn-3Mn alloys exhibit better corrosion resistance than Cu-10Ni alloy in clean synthetic seawater. Their relatively better corrosion resistance is attributed to formation of single-phased $Cu_2O$ film and incorporation of bi-valent and tri-valent cations of Mn. These alloys are more corrosion resistant than Cu-10Ni alloy in sulphide polluted synthetic seawater. Their relatively better corrosion resistance is attributed to the formation of multi-phased film containing ZnS, which is a bad conductor. This reduces the area of the film through which ionic and electronic conduction can take place. Incorporation of $Mn^{3+}$ cations in $Cu_2O$ and $Cu_2S$ lattice too has some role to play in improving corrosion resistance of manganese containing test alloys in sulphide polluted synthetic seawater.

## References


1. 'The corrosion of copper-nickel alloys 706 and 715 in flowing weawater I-effect of oxygen', D.D. Macdonald, B.C. Syrett and S.S. wing, Corrosion, 34, 9, pp289-301, 1978.

2. 'A study of de-alloying of 70Cu-30Ni commercial alloy in sulfide polluted and unpolluted seawater', A.M. Beccara et al., Corrosion Science, 32, 11, pp1263-1275, 1991.

3. 'The influence of corrosion product structure on the corrosion rate of Cu-Ni alloys', R.F. North and M.J. Pryor, Corrosion Science, 10, pp297-311, 1970.

4. 'Copper-nickle-iron alloys resistant to seawater corrosion', G.L. Baily, J. Institution of Metals, 79, pp243-292, 1951.

5. 'Behaviour of copper in artificial seawater containing sulfides', E.D. Mor and A.M. Beccaria, British Corrosion J., 10, 1, pp33-38, 1975.

6. 'Passive film on 90Cu-10Ni alloy: The mechanism of breakdown in chloride containing solutions', I. Milasev and M. Meticos-Hukovic, J. Electrochemical Society, 1432, 1, pp61-67, 1991.

7. ‘On mechanism of corrosion of Cu-9.4Ni-1.7Fe alloy in air saturated aqueous NaCl solution’, Kato et al., J. Electrochemical Society, 127, 9, pp1890-1896, 1980.

8. ‘On the effect of common pollutants on the corrosion of copper-nickel alloy in sulfide polluted seawater’, J.N. Alhajji and M.R. Reda, J. of Electrochem Society, 142, 9, pp2944-2953, 1995.

9. ‘Effects of sulfides on corrosion of Cu-Ni-Fe-Mn alloy in seawater’, Traverso P., Baccaria A.M. and Poggi G., British Corrosion Journal, 29, 2, p110-114, 1994.